Applied Catalysis B: Environmental 111–112 (2012) 150–156

Contents lists available at SciVerse ScienceDirect

Applied Catalysis B: Environmental

journal homepage: www.elsevier.com/locate/apcatb

TiO_2 mediated heterogeneous photocatalytic degradation of moxifloxacin: Operational variables and scavenger study

Xander Van Doorslaer, Philippe M. Heynderickx, Kristof Demeestere, Kevin Debevere, Herman Van Langenhove, Jo Dewulf*

Research Group EnVOC, Department of Sustainable Organic Chemistry and Technology, Faculty of Bioscience Engineering, Ghent University, Coupure Links 653, B-9000 Ghent, Belgium

ARTICLE INFO

Article history:
Received 17 August 2011
Received in revised form
23 September 2011
Accepted 25 September 2011
Available online 29 September 2011

Keywords:
Heterogeneous photocatalysis
Process parameters
Fluoroquinolone
Scavenger
Antibiotics

ABSTRACT

UV-A (485 μW cm^{-2}) TiO_2-P25 mediated heterogeneous photocatalysis is investigated as an advanced oxidation technology for the removal of the fluoroquinolone (FQ) antibiotic moxifloxacin (MOX) in aqueous solution. The goal of this work is twofold. First, the degradation kinetics are investigated by changing operational conditions during the degradation reaction. The effect of the initial MOX concentration (12.5–124.6 μmol L^{-1}), catalyst concentration (0.25–8.00 g L^{-1}), changing the oxygen concentration (0%, 20%, 100%) in the inlet gas flow (60 mL min^{-1}) and temperature (278–338 K) on the photocatalytic degradation rate is investigated. An optimal MOX degradation is attained at a catalyst concentration of 5 g L^{-1}, 298 K and air sparging at 60 mL min^{-1} resulting in an initial degradation rate of 16.2 ± 0.3 μmol L^{-1} min^{-1} and a half-life time of $t_{1/2}$ = 1.6 min.

Secondly, the aim is to gain a deeper insight of the photocatalytic degradation mechanism of MOX. Therefore an estimation of the participation of the different reactive species during the photocatalytic degradation of MOX is done using two scavengers in different concentrations. The role of hydroxyl radicals is monitored using isopropanol, and the participation of oxidative holes in the reaction mechanism is evaluated by the addition of iodine anions. The scavenger study indicates that holes are the dominant reactive species, contributing up to 63%, and that hydroxyl radicals participate for about 24% in the photocatalytic degradation of MOX. Reactive oxygen species created by conduction band electrons are probably of lower importance, <13%, during the photocatalytic degradation reaction of MOX.

1. Introduction

Fluoroquinolones (FQs) are a family of synthetic antibacterial agents with a rising popularity. The total use of quinolones as well as that of second and third generation quinolones is increasing for most European countries. One of those third generation FQs is moxifloxacin (MOX), see Fig. 1. It is worldwide approved and represented 99.5% of the European third generation quinolone use in 2003 [1,2]. Recently, pharmaceutical residues, including FQs, are often detected in natural waters [3]. Excretion, incorrect disposal, wastewater from bulk drug producers, sludge fertilisation and veterinary applications are considered as the main sources of antibiotics in surface, ground, and drinking water worldwide [4,5].

Removal of these persistent molecules in wastewater treatment plants (WWTPs) is mainly achieved by sorption processes, not by biodegradation [6]. The constant pressure of low concentrations of antibiotics together with mobile DNA from resistant bacteria present in the influent water make WWTPs a hot spot for horizontal gene transfer and selection of multiple antibiotic resistant bacteria [5]. The number of human infections caused by resistant bacteria is rapidly increasing [7]. Next to that, the inefficient removal of these persistent molecules can provoke toxic effects on fauna and flora. Acute toxicity has been described for many antibiotics but environmental relevant concentrations are more likely to cause chronic toxicity. Little is known regarding the chronic effects on aquatic organisms, making future research necessary in this field [8–10].

To prevent resistance formation and toxic effects, the removal of these antibiotics is required by physical chemical technologies prior to discharge in the environment. AOPs (advanced oxidation

Abbreviations: AOP, advanced oxidation process; CB, conduction band; DNA, desoxyribonucleine acid; DP, degradation product; FQ, fluoroquinolone; HPLC, high performance liquid chromatography; ISO, isopropanol; KI, potassium iodide; L, Langmuir; LH, Langmuir–Hinshelwood; MOX, moxifloxacin; NCR, non-captured radicals; PDA, photo diode array; ROS, reactive oxygen species; VB, valence band; WWTPs, waste water treatment plants.

* Corresponding author. Tel.: +32 9 264 59 49; fax: +32 9 264 62 43.
E-mail address: Jo.Dewulf@UGent.be (J. Dewulf).

0926-3373/$ – see front matter © 2011 Elsevier B.V. All rights reserved.
doi:10.1016/j.apcatb.2011.09.029

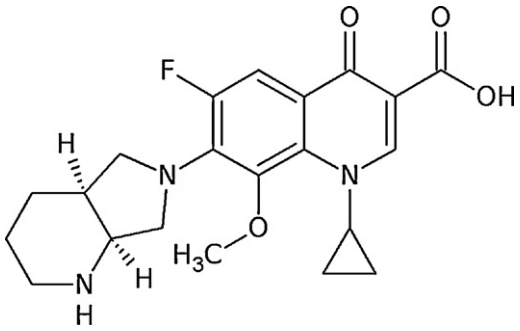

Fig. 1. Molecular structure of the FQ antibiotic moxifloxacin, $C_{21}H_{24}FN_3O_4$.

processes) like heterogeneous photocatalysis, ozonation and sonification are promising techniques to degrade persistent organic molecules [11–16].

This paper deals in a first part with the optimization of the Degussa P25 mediated photocatalytic degradation of MOX through a systematic investigation of the effect of different operational variables such as initial FQ concentration, catalyst concentration, stirring speed, inlet oxygen concentration and temperature. To the authors best knowledge, this is the first time that the effect of different operational variables is studied for the photocatalytic degradation of this third generation fluoroquinolone. Secondly, a better understanding of the contribution of some major reactive species in the photocatalytic degradation mechanism is obtained by the addition of the scavengers potassium iodide and isopropanol in different concentrations.

2. Procedures

2.1. Chemicals

Moxifloxacin·HCl, BAY12-80369, is provided by Bayer (Berlin, Germany). KH_2PO_4 (Sigma Aldrich, Bornem, Belgium, 99%), K_2HPO_4 (Acros, Geel, Belgium, ≥98%) and NaOH (Acros, Geel, Belgium) are used for pH adjustment. Isopropanol (ISO) is purchased from Fisher Scientific (Geel, Belgium, ≥99.5%) and potassium iodide (KI) from Sigma Aldrich (Bornem, Belgium, ≥99.5%). All stock and buffer solutions are prepared with deionized water and all reagents are used as received without any purification. As a photocatalyst, commercial Degussa P25 TiO_2 (Evonik, Antwerp, Belgium) is used with a BET specific surface area of $48.3 \pm 0.7\ m^2\ g^{-1}$ (TRISTAR Micromeritics, Aachen, Germany), 86.7 ± 0.6% of anatase and primary anatase and rutile particle sizes of 18.7 ± 0.1 nm and 23.3 ± 1.2 nm, respectively (Siemens D5000 scintillation counter, Bruker, Karlsruhe, Germany, $\theta = 0.02^\circ$) [17].

Oxygen (purity ≥99.9995% O_2), pure air (20 ± 1% O_2) and nitrogen (purity ≥99.8% N_2) are purchased from Air Liquide (Luik, Belgium).

2.2. Degradation experiments

Photocatalytic degradation experiments are performed in a lab scale batch reactor with a diameter and height of 7 and 10 cm, see Fig. S-1. A UV-A (485 μW cm^{-2}, 300–440 nm with main peak at 365 nm) pen ray, provided by UVP (United Kingdom), is used as the light source during the photocatalytic degradation experiments. The same methodology is applied as reported in Van Doorslaer et al. [18]. The solution is continuously stirred and sparged in the dark for 30 min to attain adsorption/desorption equilibrium. During degradation samples are taken at regular time intervals, filtered and analyzed by HPLC–PDA. Investigated operational variables are listed in Table 1.

Table 1
Experimental conditions applied during heterogeneous photocatalytic degradation of MOX.

Process variable	Unit	Value
Initial concentration, $C_{MOX,0}$	μM	12.5, 24.9, 37.4, 49.9, 62.3 and 124.6
Temperature	K	278, 288, 298, 308, 318 and 338
pH	–	7
Stirring speed 1, 2 and 3	rps[a]	2.3, 7.9 and 13.2
Reactor volume	mL	200
Catalyst loading, C_{cat}	g L^{-1}	0.25, 0.5, 1, 3, 5 and 8
Oxygen, air, nitrogen flow	mL min^{-1}	60
Buffer concentration	mM	10
Light intensity UV-A at 3 cm[b]	μW cm^{-2}	485
ISO concentration	μmol L^{-1}	37.4, 374, 3740, 37.4×10^3, 74.8×10^3 and 18.7×10^4
KI concentration	μmol L^{-1}	3.74, 37.4, 374, 3740 and 7480

[a] rps: rounds per second.
[b] Distance measured from light source.

2.3. Effect of radical inhibitors

An estimate of the contribution of hydroxyl radicals (HO•) and positive holes (h+) during the heterogeneous photocatalytic degradation of MOX is determined by adding different concentrations of ISO and KI to the reaction solution, see Table 1. Adsorption experiments were performed to determine if the added scavenger affected the MOX adsorption on the catalyst surface. An initial MOX concentration ($C_{MOX,0}$) of 37.4 μmol L^{-1}, catalyst concentration (C_{cat}) of 1 g L^{-1} and a reaction temperature of 298 K are applied. If scavenger addition did not influence MOX adsorption degradation reactions are performed under the same conditions while the solution is continuously stirred (13.2 rps) and sparged with dry air (60 mL min^{-1}).

2.4. HPLC–PDA analysis

MOX concentrations are measured by liquid chromatography (HPLC) coupled to a photodiode array detector (PDA, Surveyor, Thermo Scientific, USA). A Luna C18(2) column (150 mm × 3.0 mm, 3 μm, Phenomenex, USA) with a mobile phase containing 86% water (0.1% formic acid) and 14% acetonitrile is used for the chromatographic analysis of MOX. Quantification of MOX is done at 296.0 ± 4.5 nm.

3. Results and discussion

The effect of pH is presented in previously published work [18]. It is concluded that neutral conditions are preferred above acid or alkaline conditions during photocatalytic degradation of MOX. Therefore pH 7 is applied for all the degradation experiments presented in this work. The pH is controlled by a phosphate buffer (see Section 2.1) and no change in pH could be observed during the photocatalytic degradation of MOX.

3.1. Initial MOX concentration

The effect of the initial MOX concentration ($C_{MOX,0}$) was studied in the range 12.5–124.6 μmol L^{-1} at 5 g L^{-1} TiO_2 loading. From the total amount of MOX added, a part is adsorbed on the TiO_2 surface until adsorption equilibrium is attained. By measuring the aqueous concentrations ($C_{MOX,l,eq,0}$) at adsorption–desorption equilibrium after the addition of different initial MOX concentrations, an adsorption isotherm is determined. The isotherm fits the Langmuir adsorption model well ($R^2 = 0.998$). The Langmuir adsorption isotherm shows that under the highest initial FQ concentration

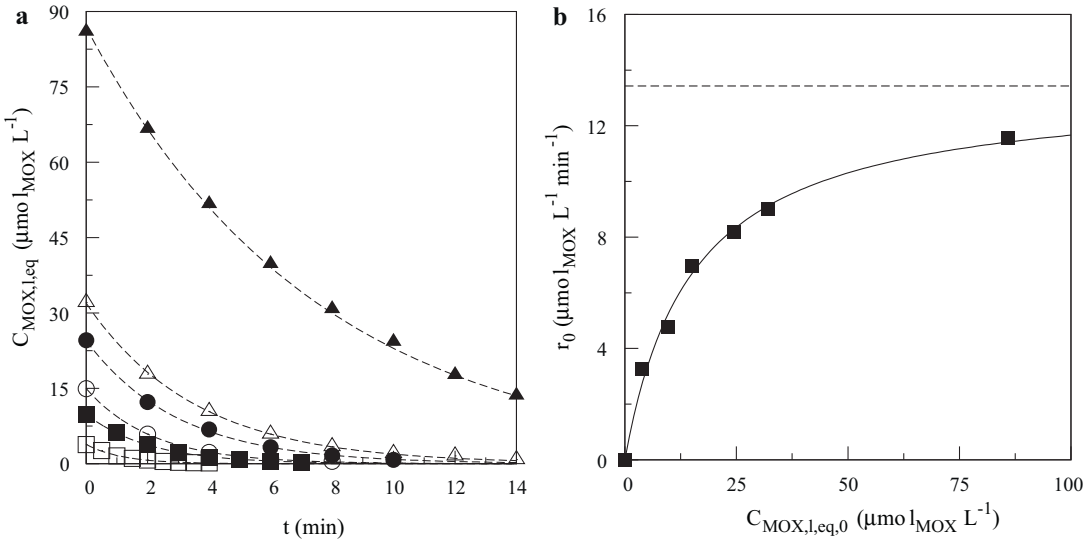

Fig. 2. a: Photocatalytic degradation of (▲) 124.6 µM, (△) 62.3 µM, (●) 49.9 µM, (○) 37.4 µM, (■) 24.9 µM and (□) 12.5 µM MOX at pH 7, 298 K, 5 g L^{-1} TiO_2, air sparging (60 mL min^{-1}) and stirring speed 13.2 rps. Dashed lines represent the best fitting polynomic function to connect the experimental data points. b: Initial degradation rate, r_0, of MOX (µmol$_{MOX}$ L^{-1} min^{-1}) as a function of initial equilibrium MOX concentration, $C_{MOX,l,eq,0}$, (µmol$_{MOX}$ L^{-1}) deduced from a. The full line is obtained by fitting the Langmuir–Hinshelwood equation to the experimental data points (R^2 = 0.998). The modeled maximal initial degradation rate is represented by the dashed asymptotic line.

used, no monolayer of adsorbed MOX is attained on the catalyst surface (Fig. S-2).

The total photocatalytic degradation time is longer at higher initial MOX concentrations, see Fig. 2a. As the oxidation reaction proceeds, a smaller fraction of the TiO_2 particle surface is covered by MOX as it is degraded. Evidently, a decrease in the photocatalytic degradation rate is to be expected with increasing irradiation time [19]. Therefore, to compare different situations, initial degradation rates are determined by fitting a polynomic function to the experimental data and taking the tangent in $t = 0$. Initial degradation rates for the photocatalytic degradation of MOX as a function of the initial equilibrium MOX concentration ($C_{MOX,l,eq,0}$) are shown in Fig. 2b.

The Langmuir–Hinshelwood (LH) kinetics, see Eq. (1), is the most commonly used kinetic expression to explain the kinetics of heterogeneous photocatalytic processes of various organics by TiO_2 [20,21]:

$$r_0 = -\frac{dC_{MOX,l,eq,0}}{dt} = \frac{k_r K_{LH} C_{MOX,l,eq,0}}{1 + K_{LH} C_{MOX,l,eq,0}} \quad (1)$$

where r_0 is the initial degradation rate, $C_{MOX,l,eq,0}$ the MOX concentration in the liquid phase after equilibrium (µmol L^{-1}), k_r the reaction rate coefficient (µmol L^{-1} min^{-1}), and K_{LH} the LH adsorption coefficient (L µmol^{-1}). The linear transformation of Eq. (1) gives a rate coefficient, k_r, and an adsorption coefficient, K_{LH}, both with its 95% confidence interval, of 13.4 ± 1.9 µmol L^{-1} min^{-1} and 0.066 ± 0.008 µmol L^{-1}, respectively.

The initial degradation rate increases from 3.2 to 11.6 µmol$_{MOX}$ L^{-1} min^{-1} with increasing initial equilibrium MOX concentrations from 3.8 to 86.0 µmol L^{-1}, respectively. At higher $C_{MOX,l,eq,0}$ concentrations, the initial degradation rate levels off since the complete coverage of the semiconductor surface is approached. The maximum initial degradation rate of 13.4 µmol L^{-1} min^{-1} is theoretically attained when the MOX monolayer is formed, which is visualized by the dashed line. A similar trend is noticed for the P25 mediated photocatalytic degradation of norfloxacin and ofloxacin [19,22].

3.2. Catalyst concentration and stirring speed

Preliminary suspension experiments revealed that sedimentation occurs for TiO_2 P25 catalyst concentrations varying from 0.25 to 8 g L^{-1} under the slowest stirring regime, 2.3 rps. No sedimentation is observed using stirring speeds greater than 7.9 rps, see Fig. S-3 in supplementary content. Degradation experiments with the lowest stirring speed are not performed due to the inefficient use of catalyst.

It is worth noticing that the initial equilibrium concentration of MOX in the liquid phase ($C_{MOX,l,eq,0}$) is not the same for every catalyst concentration because of the higher fraction of adsorbed MOX at higher catalyst concentrations, see Fig. 3a. Therefore, it is difficult to compare solely the effect of the investigated variable catalyst concentration due to the fact that changing initial equilibrium concentrations in the liquid phase also alters the initial MOX degradation rate r_0 (see Section 3.1). A possible solution is to express the degradation of MOX in total moles of MOX in the reactor as a function of time. Adsorption experiments performed with different catalyst concentrations and the same initial MOX concentration enable the calculation of the amount of MOX adsorbed on TiO_2 for every $C_{MOX,l,eq,t}$ during a degradation experiment. Degradation curves are now expressed as the total amount of moles MOX left in the reactor, both in liquid phase and in adsorbed phase, as function of time, see Fig. 3b. The initial photocatalytic degradation rate of MOX deduced at $t = 0$ is denoted as r_0^*. This procedure is from now on applied for all the operational variables studied in this paper.

Using the initial degradation rates as determined in Fig. 3b, the effect of the photocatalyst concentration on r_0^* is examined, see Fig. 4. An optimal catalyst loading of 5 g L^{-1} TiO_2 is observed for both stirring speeds. A more vigorous stirring regime results in a higher initial degradation rate probably due to the increase in turbulence.

Dosing more catalyst to the reaction solution below the optimal loading results in a higher initial degradation rate for both stirring speeds. This may be attributed to the higher amount of total active surface area, i.e., a larger number of active surface sites and a more pronounced light absorption when the added catalyst mass increases [23]. It is assumed that the geometric catalyst surface

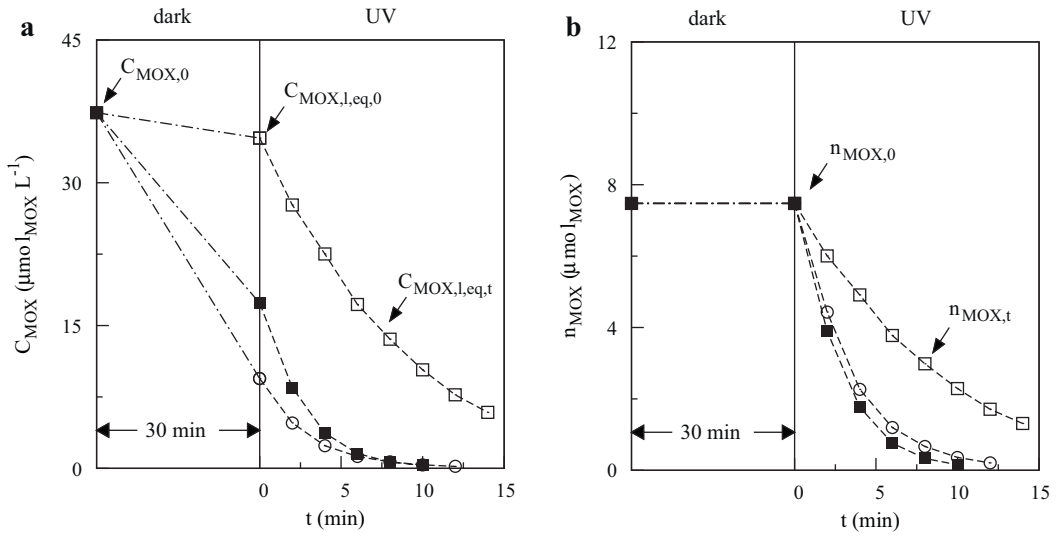

Fig. 3. a: Concentration profile of aqueous MOX in the dark period and in the UV period for the catalyst loadings (□) 0.25 g L^{-1}, (■) 3 g L^{-1} and (○) 8 g L^{-1} at pH 7, 37.4 μmol$_{MOX}$ L^{-1}, 298 K, air sparging (60 mL min^{-1}) and stirring speed 13.2 rps. b: The total amount of moles of MOX present in the reactor in the dark period and in the UV period for the catalyst loadings (□) 0.25 g L^{-1}, (■) 3 g L^{-1} and (○) 8 g L^{-1} at pH 7, 37.4 μmol$_{MOX}$ L^{-1}, 298 K, air sparging (60 mL min^{-1}) and stirring speed 13.2 rps. Initial degradation rates, r_0^* (μmol$_{MOX}$ L^{-1} min^{-1}), are determined by plotting the tangent at $t = 0$, this is after equilibration in the dark period. The interrupted dashed lines express the adsorption equilibration time of MOX and the full dashed lines represent the photocatalytic degradation of MOX in the UV period and connect the experimental data points.

area and the absorption of light by TiO_2 are limiting factors when working below the optimal catalyst loading [24].

Above the optimal catalyst loading, the initial degradation rate decreases with higher catalyst concentrations. Different factors may influence the degradation rate when working above optimal conditions: (a) increased turbidity and opacity of the solution with scattering phenomena reducing the light transmission through the solution (shielding effect) [25], (b) agglomeration of the catalyst due to particle–particle interactions resulting in the loss of active surface sites [22], (c) a higher catalyst dosage results in a lower degree of surface coverage, and (d) deactivation of the originally activated TiO_2 particles through collision with ground state catalyst particles, see Eq. (2):

$$TiO_2^* + TiO_2 \rightarrow TiO_2^{\#} + TiO_2 \quad (2)$$

where TiO_2^* is the TiO_2 with active species adsorbed on the surface and $TiO_2^{\#}$ the ground state form of TiO_2 [26].

The dependency of the optimal TiO_2 loading on both the photoreactor geometry and the nature of the compound, makes it difficult to compare different optimum catalyst loadings obtained in different studies. Optimal catalyst concentrations reported in literature for Degussa TiO_2 P25 range from 0.1 to 5.0 g L^{-1} [27].

3.3. Oxygen concentration

The effect of sparging pure oxygen, pure air, nitrogen and passive diffusion (no sparging) of ambient air on the initial degradation rate of the photocatalytic degradation of MOX is presented in Fig. 5. MOX

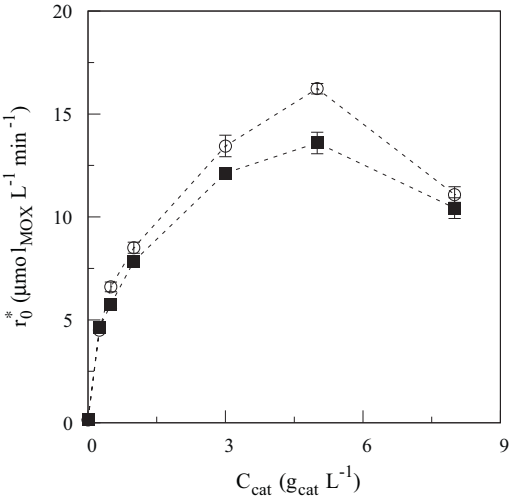

Fig. 4. Initial degradation rate, r_0^* (μmol$_{MOX}$ L^{-1} min^{-1}) as a function of catalyst loading (g L^{-1}) for the stirring speeds (■) 7.9 rps and (○) 13.2 rps at pH 7, 37.4 μmol$_{MOX}$ L^{-1}, 298 K and air sparging (60 mL min^{-1}). Standard deviations, represented as error bars, are based on replicate measurements, $n_{rep} = 3$. Dashed lines are plotted to guide the eye.

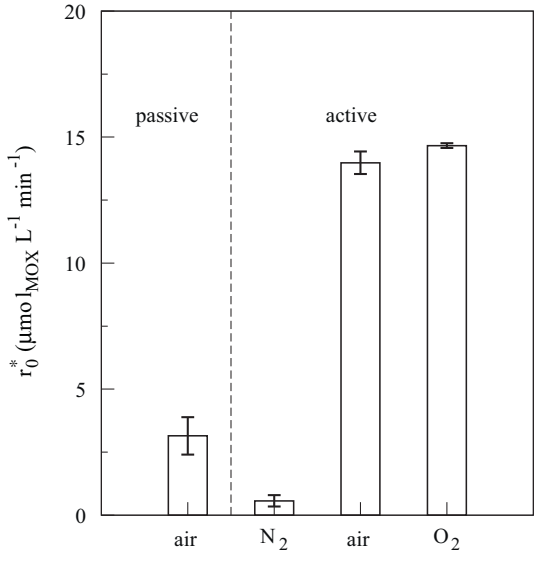

Fig. 5. Initial degradation rate, r_0^* (μmol$_{MOX}$ L^{-1} min^{-1}) as a function of oxygen supply (20% passive, 0%, 20% and 100%) at pH 7, 5.0 g L^{-1} TiO_2, 37.4 μmol$_{MOX}$ L^{-1}, 298 K and stirring speed 13.2 rps. The active part is sparged with a flow of 60 mL min^{-1}, the passive part is not sparged but kept open to the atmosphere during reaction. Error bars are based on replicate measurements ($n_{rep} = 3$).

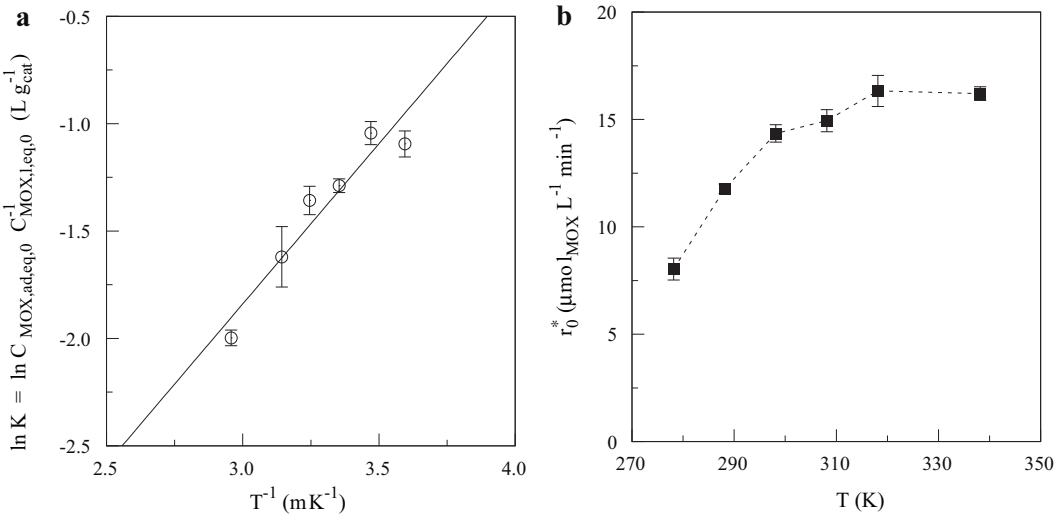

Fig. 6. a: Linearisation of the van't Hoff equation for the temperature range 278–338 K. Given error bars are based on triplicate measurements. b: Initial degradation rate, r_0^* ($\mu mol_{MOX}\ L^{-1}\ min^{-1}$), of MOX as a function of reaction temperature at pH 7, 5 g L^{-1} TiO_2, 37.4 $\mu mol_{MOX}\ L^{-1}$, stirring speed 13.2 rps and air sparging (60 mL min^{-1}). Error bars are based on replicate measurements, n_{rep} = 3. Dashed line is plotted to guide the eye.

degrades significantly slower under N_2 sparging compared to pure oxygen and air. Since oxygen free environments inhibit the photocatalytic degradation of organic compounds completely, there is probably still a residual amount of oxygen available in the reaction solution being responsible for the observed slow MOX degradation rate under N_2 sparging [28]. Oxygen adsorbed on the surface of TiO_2 prevents the recombination process by trapping the conduction band electrons with the formation of superoxide radical ions, $O_2^{\bullet -}$.

The formation of this superoxide radical ion can result in the formation of more reactive oxygen species (ROS) like peroxide radicals [29]. Oxygen has no negative effect on the adsorption of the compound since the reduction reaction takes place at a different location from where oxidation occurs [30].

Comparing the sparging of dry air and pure oxygen a 5% increase in the initial degradation rate of MOX is observed when applying pure oxygen. The same trend is noticed during the degradation of other organic compounds using heterogeneous photocatalysis [28,30,31]. The use of ambient air is therefore a promising alternative for future applications in photocatalytic degradation reactions.

Sparging the solution during the photocatalytic degradation is nonetheless necessary. Experiments performed with passive diffusion of ambient air show that the oxygen diffusion is too slow to prevent the electron–hole recombination process. The initial degradation rate decreases with 77% in comparison to active air diffusion due to the slow oxygen diffusion towards the reaction solution.

3.4. Temperature

Adsorption experiments performed under temperatures ranging from 278 up to 338 K show that the adsorption of MOX decreases with a rising solution temperature. The enthalpy of the MOX adsorption on TiO_2 is calculated to amount -16.8 ± 1.9 kJ mol^{-1} by using the van't Hoff equation, which is an indirect method to calculate thermodynamic adsorption parameters at solid–solution interfaces (Fig. 6a). The negative value of the adsorption enthalpy, ΔH°, indicates the exothermic nature of the process. The magnitude gives an idea about the type of adsorption, which is mainly physical or chemical. Physisorption processes usually have energies in the range of 10–40 kJ mol^{-1} while higher adsorption enthalpies of 100–500 kJ mol^{-1} suggest chemisorption [32,33]. The calculated adsorption enthalpy of MOX in this study indicates the physisorbed nature of the adsorption process on TiO_2. Similar values are obtained for phenol adsorption on activated carbon and cyanide adsorption on TiO_2 [33,34].

The influence of the applied reaction temperature on the initial degradation rate of MOX is presented in Fig. 6b. In this figure, two regions can be defined which are probably the result of two counter effects, namely the decreasing MOX adsorption at higher temperatures and the faster diffusion and reaction kinetics with increasing temperature. Below a reaction temperature of 298 K the increase in diffusion rate and kinetics have the upper hand, resulting in a higher initial degradation rate with an increasing temperature. Above 298 K a leveling off appears and the expected increase of the initial degradation rate with increasing temperature is possibly compensated by the decrease in MOX adsorption [35–37], the decrease in oxygen solubility with higher working temperatures [31,38], and/or the faster recombination of charge carriers [30,39]. According to Geng and Duan [38], the oxygen concentration can decrease from 13 to 5 mg O_2 L^{-1} with temperatures ranging from 278 to 338 K. The importance of oxygen is discussed in the previous paragraph.

3.5. Effect of radical inhibitors

Two scavengers, ISO and KI, were added to the reaction solution in order to capture reactive species during a photocatalytic reaction. Adsorption experiments for different scavenger concentrations of ISO and KI show that no interference is noticed for the applied KI concentrations up to 3.74 mmol L^{-1} and that ISO did not interfere up to a concentration of 37.4 mmol L^{-1}. Applying higher KI and ISO concentrations, as mentioned in Table 1, interferes with MOX adsorption. To compare the photocatalytic degradation reaction of MOX with and without the addition of scavenger, degradation reactions are performed only in these cases where no interference with the MOX adsorption is noticed.

3.6. Isopropanol

ISO is known to be a good hydroxyl radical scavenger with a reaction constant (k) of 1.9×10^9 L mol^{-1} s^{-1} and is used to discriminate between direct oxidation with positive holes and the degradation with hydroxyl radicals in solution [40–42]. Though direct oxidation of short aliphatic alcohols by photogenerated holes occurs, it was

Table 2
Percentage of inhibition due to the scavengers KI and ISO, and the percentage of contribution for the photocatalytic holes and hydroxyl radicals during the photocatalytic degradation of MOX under the conditions mentioned in Section 2.3 with α (mol mol^{-1}) the ratio scavenger over MOX concentration.

α_{KI}	α_{ISO}	Percentage of inhibition		Percentage of contribution		
		KI (%)[a]	ISO (%)[a]	h+ (%)[b]	HO• (%)[b]	NCR (%)[b]
0	0	0	0	0	100	
0.1	0.1	12.9 ± 0.2	n.d.[c]	n.d.	n.d.	n.d.
1	1	13.1 ± 0.2	5.1 ± 0.1	8.0 ± 0.2	5.1 ± 0.1	86.9 ± 0.2
10	10	27.9 ± 0.3	6.0 ± 1.1	21.9 ± 1.1	6.0 ± 1.1	72.1 ± 1.6
100	100	73.3 ± 1.1	10.3 ± 0.1	63.0 ± 1.1	10.3 ± 0.1	26.7 ± 1.1
1000	1000	n.d.	23.6 ± 0.2	n.d.	23.6 ± 0.2	n.d.
100	1000	73.3 ± 1.1	23.6 ± 0.2	63.0 ± 1.1	23.6 ± 0.2	13.4 ± 1.1

[a] Confidence intervals (95%) are reported.
[b] Standard deviations are based on error propagation.
[c] Not determined.

considered negligible because they have a very weak adsorption on TiO_2 surfaces in aqueous media [40]. Different concentrations of ISO were dosed to evaluate the effect on the heterogeneous photocatalytic degradation of MOX, see Fig. 7.

The bimolecular rate constant of MOX with a hydroxyl radical is estimated to be 1.38×10^{10} L mol^{-1} s^{-1}, which is the mean value of the lowest (norfloxacin) and highest (ciprofloxacin) value of fluoroquinolones found in literature [43,44]. Dividing the reaction rates of ISO and MOX with hydroxyl radicals, Eq. (3) is deduced

$$\gamma_{ISO} = \frac{r_{0,ISO}}{r_{0,MOX}} = \frac{k_{0,ISO}C_{0,ISO}C_{HO\bullet}}{k_{0,MOX}C_{0,MOX}C_{HO\bullet}} = 0.14\frac{C_{0,ISO}}{C_{0,MOX}} = 0.14\alpha_{ISO} \quad (3)$$

with γ_{ISO} the ratio of the reaction rate of ISO and MOX with hydroxyl radicals and α_{ISO} the ratio of ISO over MOX concentration. Altering the ISO to MOX concentration ratio within the experimental ranges applied in this study results in a γ from 0.14 to 140. A first significant decrease of the initial degradation rate was noticed at α_{ISO} = 100. Here, the initial degradation rate of ISO with hydroxyl radicals is 14 times higher than the one of MOX due to its higher concentration.

At α_{ISO} = 1000 a drop of only 25% in initial degradation rate was noticed. This relatively small decrease in initial degradation rate with a high scavenger concentration can be an indication that hydroxyl radicals in solution have a moderate contribution in the photocatalytic degradation reaction mechanism of MOX.

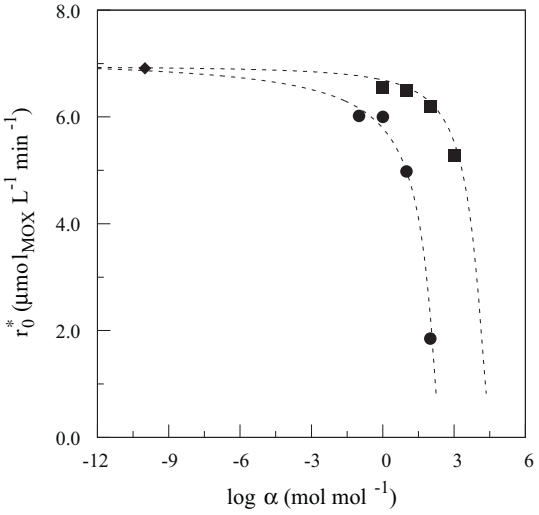

Fig. 7. Initial degradation rate, r_0^* (μmol$_{MOX}$ L^{-1} min^{-1}), of MOX as a function of different (■) ISO and (●) KI concentrations expressed as the ratio α. Experiments are performed at 37.4 μM$_{MOX}$, pH 7, 298 K, 1.0 g L^{-1} TiO_2, stirring speed 13.2 rps and air sparging of 60 mL min^{-1}. Initial degradation rate with no added scavenger is presented with (♦). Dashed lines are plotted to guide the eye.

ISO concentrations above α_{ISO} = 1000 negatively influence the adsorption process of MOX up to 40% which makes the decrease in initial degradation rate a combination of inhibition and lowered MOX adsorption.

3.7. Potassium iodide

The iodide ion is used to evaluate the contribution of both photogenerated holes and hydroxyl radicals, bimolecular rate constant k of 1.1×10^{10} L mol^{-1} s^{-1} [45], in the photocatalytic degradation of MOX. Valence band holes and hydroxyl radicals are easily captured by I^- [40,46,47]. Different concentrations of KI were applied during the heterogeneous photocatalytic degradation of MOX, see Fig. 7. Applying an α_{KI} of 100 a decrease of 80% in the initial degradation rate can be noticed. When applying KI concentrations above α_{KI} = 100 a negative influence on the adsorption process of MOX up to 75% is noticed which makes the decrease in initial degradation rate a combination of inhibition and lowered MOX adsorption as noticed with ISO.

The greater inhibition of the reaction through KI compared to ISO at lower scavenger concentrations gives an indication that photogenerated holes play a more important role in the photodegradation of MOX under UV-A light irradiation than hydroxyl radicals [47,48].

Relevant contribution estimates are obtained for the different active species during the photocatalytic degradation of MOX at different scavenger concentrations, see Table 2. Knowing that ISO scavenges hydroxyl radicals and KI both holes and hydroxyl radicals, one can calculate the minimum percentage of holes and hydroxyl radicals which participate in the photocatalytic degradation of MOX. If 100% is the total amount of reactive species, then the abstraction of the holes and hydroxyl radicals result in the amount of non-captured radicals (NCR), which can be holes, hydroxyl radicals and reactive oxygen species (ROS). More radicals are captured with increasing scavenger concentrations. The results in Table 2 indicate that photocatalytic holes and hydroxyl radicals are the two reactive species which are probably responsible for the greatest part in the photocatalytic breakdown of MOX, 63% and 24%, respectively. Since KI and ISO are not used to scavenge ROS during the photocatalytic degradation of MOX, they are enclosed in the NCR and results in the fact that ROS are probably responsible for equal or less than 13% of the photocatalytic degradation. These radicals have therefore a minor contribution in the reaction pathway of the antibiotic moxifloxacin [40,49].

4. Conclusions

New data and insights are obtained with respect to the kinetics and mechanism of the TiO_2 mediated heterogeneous photocatalytic degradation of a third generation fluoroquinolone, moxifloxacin. A

better understanding of the kinetics are obtained by investigating a wide set of operational variables. The photocatalytic degradation of MOX can be described by the Langmuir–Hinshelwood kinetics and an optimal catalyst loading is observed at 5.0 g L^{-1} with a higher initial degradation rate at a higher stirring speed (13.2 rps). Applying pure oxygen (60 mL min^{-1}) does not result in a major increase in initial degradation rate comparing to pure air, but aeration is nonetheless necessary since passive diffusion of oxygen from the ambient air to the solution is too slow. The small increase (<10% at 338 K) in initial degradation rate above 298 K is a clear indication that ambient temperature is sufficient for the photocatalytic degradation reaction of MOX.

Estimated amounts of the different reactive species during the photocatalytic degradation of MOX are obtained using two scavengers at different concentrations. Photogenerated holes have a minimum contribution of 63% in the photocatalytic degradation of MOX. This indicates that holes are mainly responsible for the oxidation of MOX and that only a small amount of the degradation can be attributed to hydroxyl radicals, i.e., 24%. The amount of non-captured radicals reveals that the reactive oxygen species like superoxide radicals, have a negligible part in the photocatalytic degradation pathway of MOX, i.e., ≤13%.

Nomenclature

Roman symbols

C	concentration, mol L^{-1}
K	adsorption coefficient, L μmol^{-1}
k_r	rate coefficient, see Eq. (1), L mol^{-1} min^{-1}
k	rate constant, see Eq. (3), L mol^{-1} s^{-1}
n_{rep}	number of repetitions, –
r_0	initial degradation rate, μmol L^{-1} min^{-1}
r_0^*	initial degradation rate, μmol L^{-1} min^{-1}

Greek symbols

α	ratio of scavenger concentration to MOX concentration, see Eq. (3), mol mol^{-1}
γ	ratio of degradation rate, see Eq. (3), mol mol^{-1}

Superscripts

*	index in Eq. (2)
#	index in Eq. (2)

Subscripts

cat	catalyst
eq	equilibrium
l	liquid phase

Appendix A. Supplementary data

Supplementary data associated with this article can be found, in the online version, at doi:10.1016/j.apcatb.2011.09.029.

References

[1] M. Ferech, S. Coenen, S. Malhotra-Kumar, K. Dvorakova, E. Hendrickx, C. Suetens, H. Goossens, E.P. Grp, J. Antimicrob. Chemother. 58 (2006) 423–427.
[2] F. Van Bambeke, J.M. Michot, J. Van Eldere, P.M. Tulkens, Clin. Microbiol. Infect. 11 (2005) 256–280.
[3] K. Kummerer, J. Environ. Manage. 90 (2009) 2354–2366.
[4] J. Fick, H. Soderstrom, R.H. Lindberg, C. Phan, M. Tysklind, D.G.J. Larsson, Environ. Toxicol. Chem. 28 (2009) 2522–2527.
[5] O.A.H. Jones, N. Voulvoulis, J.N. Lester, Crit. Rev. Toxicol. 34 (2004) 335–350.
[6] B. Li, T. Zhang, Environ. Sci. Technol. 44 (2010) 3468–3473.
[7] P. Collignon, J.H. Powers, T.M. Chiller, A. Aidara-Kane, F.M. Aarestrup, Clin. Infect. Dis. 49 (2009) 132–141.
[8] S. Kar, K. Roy, Chemosphere 81 (2010) 738–747.
[9] G. Carlsson, S. Orn, D.G.J. Larsson, Environ. Toxicol. Chem. 28 (2009) 2656–2662.
[10] A.A. Robinson, J.B. Belden, M.J. Lydy, Environ. Toxicol. Chem. 24 (2005) 423–430.
[11] B. De Witte, H. Van Langenhove, K. Demeestere, K. Saerens, P. De Wispelaere, J. Dewulf, Chemosphere 78 (2010) 1142–1147.
[12] E. De Bel, J. Dewulf, B. De Witte, H. Van Langenhove, C. Janssen, Chemosphere 77 (2009) 291–295.
[13] T. Paul, M.C. Dodd, T.J. Strathmann, Water Res. 44 (2010) 3121–3132.
[14] M.N. Abellan, J. Gimenez, S. Esplugas, Catal. Today 144 (2009) 131–136.
[15] T.G. Vasconcelos, K. Kummerer, D.M. Henriques, A.F. Martins, J. Hazard. Mater. 169 (2009) 1154–1158.
[16] P.M. Heynderickx, K. Demeestere, J. Dewulf, B. De Witte, H. Van Langenhove, J. Adv. Oxid. Technol. 14 (2011) 71–80.
[17] R.A. Spurr, H. Myers, Anal. Chem. 29 (1957) 760–762.
[18] X. Van Doorslaer, K. Demeestere, P.M. Heynderickx, H. Van Langenhove, J. Dewulf, Appl. Catal. B-Environ. 101 (2011) 540–547.
[19] M.M. Haque, M. Muneer, J. Hazard. Mater. 145 (2007) 51–57.
[20] K.V. Kumar, K. Porkodi, F. Rocha, Catal. Commun. 9 (2008) 82–84.
[21] K. Demeestere, J. Dewulf, H. Van Langenhove, Crit. Rev. Environ Sci. Technol. 37 (2007) 489–538.
[22] I. Michael, E. Hapeshi, C. Michael, D. Fatta-Kassinos, Water Res. 44 (2010) 5450–5462.
[23] L. Wei, C. Shifu, Z. Wei, Z. Sujuan, J. Hazard. Mater. 164 (2009) 154–160.
[24] E. Evgenidou, K. Fytianos, I. Poulios, J. Photochem. Photobiol. A 175 (2005) 29–38.
[25] K. Mehrotra, G.S. Yablonsky, A.K. Ray, Ind. Eng. Chem. Res. 42 (2003) 2273–2281.
[26] B. Neppolian, H.C. Choi, S. Sakthivel, B. Arabindoo, V. Murugesan, J. Hazard. Mater. 89 (2002) 303–317.
[27] S. Qourzal, M. Tamimi, A. Assabbane, Y. Alt-Ichou, J. Colloid Interface Sci. 286 (2005) 621–626.
[28] T.A. McMurray, P.S.M. Dunlop, J.A. Byrne, J. Photochem. Photobiol. A-Chem. 182 (2006) 43–51.
[29] N.P. Xekoukoulotakis, C. Drosou, C. Brebou, E. Chatzisymeon, E. Hapeshi, D. Fatta-Kassinos, D. Mantzavinos, Catal. Today 161 (2011) 163–168.
[30] M.N. Chong, B. Jin, C.W.K. Chow, C. Saint, Water Res. 44 (2010) 2997–3027.
[31] S. Malato, P. Fernandez-Ibanez, M.I. Maldonado, J. Blanco, W. Gernjak, Catal. Today 147 (2009) 1–59.
[32] A.H. Berger, A.S. Bhown, Energy Procedia 4 (2011) 562–567.
[33] J.R. Parga, V. Vazquez, H.M. Casillas, J.L. Valenzuela, Chem. Eng. Technol. 32 (2009) 1901–1908.
[34] P. Canizares, M. Carmona, O. Baraza, A. Delgado, M.A. Rodrigo, J. Hazard. Mater. 131 (2006) 243–248.
[35] E. Evgenidou, K. Fytianos, I. Poulios, Appl. Catal. B-Environ. 59 (2005) 81–89.
[36] J.M. Herrmann, Appl. Catal. B-Environ. 99 (2010) 461–468.
[37] W.T. Tsai, M.K. Lee, T.Y. Su, Y.M. Chang, J. Hazard. Mater. 168 (2009) 269–275.
[38] M. Geng, Z. Duan, Geochim. Cosmochim. Acta 74 (2010) 5631–5640.
[39] L. Rideh, A. Wehrer, D. Ronze, A. Zoulalian, Ind. Eng. Chem. Res. 36 (1997) 4712–4718.
[40] Y.X. Chen, S.Y. Yang, K. Wang, L.P. Lou, J. Photochem. Photobiol. A 172 (2005) 47–54.
[41] R. Palominos, J. Freer, M.A. Mondaca, H.D. Mansilla, J. Photochem. Photobiol. A 193 (2008) 139–145.
[42] X.W. Zhang, D.D. Sun, G.T. Li, Y.Z. Wang, J. Photochem. Photobiol. A 199 (2008) 311–315.
[43] T.C. An, H. Yang, W.H. Song, G.Y. Li, H.Y. Luo, W.J. Cooper, J. Phys. Chem. A 114 (2010) 2569–2575.
[44] T.C. An, H. Yang, G.Y. Li, W.H. Song, W.J. Cooper, X.P. Nie, Appl. Catal. B-Environ. 94 (2010) 288–294.
[45] G.V. Buxton, C.L. Greenstock, W.P. Helman, A.B. Ross, J. Phys. Chem. Ref. Data 17 (1988) 513–886.
[46] S.T. Martin, A.T. Lee, M.R. Hoffmann, Environ. Sci. Technol. 29 (1995) 2567–2573.
[47] K. Ishibashi, A. Fujishima, T. Watanabe, K. Hashimoto, J. Photochem. Photobiol. A 134 (2000) 139–142.
[48] A.L. Giraldo, G.A. Peñuela, R.A. Torres-Palma, N.J. Pino, R.A. Palominos, H.D. Mansilla, Water Res. 44 (2010) 5158–5167.
[49] H. Yang, G.Y. Li, T.C. An, Y.P. Gao, J.M. Fu, Catal. Today 153 (2010) 200–207.